Research Article

Dong Tian-Shun, Wang Ran, Li Guo-Lu*, and Liu Ming*

Failure mechanism and acoustic emission signal characteristics of coatings under the condition of impact indentation

https://doi.org/10.1515/htmp-2019-0007
Received Dec 15, 2018; accepted Jan 10, 2019

Abstract: In this work, the substrate, NiCr coating, Al_2O_3 coating with NiCr undercoating and Al_2O_3 coating were tested by an impact indentation device equipped with an acoustic emission (AE) detection equipment. The surface morphology, dimension, cross-sectional image, 3D topography of indention and bonding strength of coatings were analyzed. The failure mechanism and AE signal characteristics of the coatings under impact were studied. The results demonstrate that the failure mode of NiCr coating was dominated by interface cracking, and that of Al_2O_3 coating is fracture and accompanied by a small amount of interface cracking, while Al_2O_3 coating with NiCr undercoating possesses common characteristics of the first two. The energy counting and wave voltage of AE signal were more sensitive to the bonding strength of coating in the impact process, which can be used to characterize the bonding strength of coating.

Keywords: Coating; bonding strength; impact indentation method; acoustic emission

1 Introduction

Thermal spraying technique has been widely used in various mechanical parts as a surface modification technique. Because of the combination between the coating and the substrate is mainly mechanical bonding, the bonding strength of coating is usually taken as one of the most important indexes to evaluate the coating's quality. The methods available today to test bonding strength of coating are mainly tensile method [1], scratch method [2], bending method [3], shearing method [4], etc. However, all of these methods need to prepare specialized samples for indirect test on the testing machine, so they cannot be used for field direct test.

Song [5] proposed that an ideal method to detect the bonding strength of coating needs to meet at least two basic conditions: one is the model that characterizes the failure between the coating and the substrate; the other is the characteristic parameters which can response to the failure of the coating. Based on this idea, we have adopted the approach of "static load indentation + AE detection" to measure the bonding strength of coating, which can provide theoretical basis and experimental support for "indentation method +AE detection "[6–8]. In previous research, which we have carried out, we demonstrated that the process of static load indentation was too moderate to induce the failure of the coating effectively, which led to the extracted signal showing greater dispersion. Therefore, the impact indentation method was adopted in this work, which was easy to induce the failure of the coating and reduce the dispersion of the AE signals.

In this work, high efficiency supersonic plasma spraying system was employed to prepare three types of coatings, namely the metal coating (NiCr), ceramic coating with the undercoating (NiCr as transition coating and Al_2O_3 as working coating) and Al_2O_3 coating, whose bonding strength varies greatly. Subsequently, impact indentation method was used to evaluate the bonding strength of the above coatings, whereupon the relationship between the failure mechanism of coatings and acoustic emission (AE) signal characteristics under impact condition were studied. This study has important reference value for coating field detection.

***Corresponding Author: Li Guo-Lu:** School of Materials Science and Engineering, Hebei University of Technology, Tian jin 300130, China; Email: liguolu0305@163.com
***Corresponding Author: Liu Ming:** National Key Laboratory for Remanufacturing, Academy of Armored Forces Engineering, Beijing 100072, China; Email: hzaam@163.com
Dong Tian-Shun, Wang Ran: School of Materials Science and Engineering, Hebei University of Technology, Tian jin 300130, China

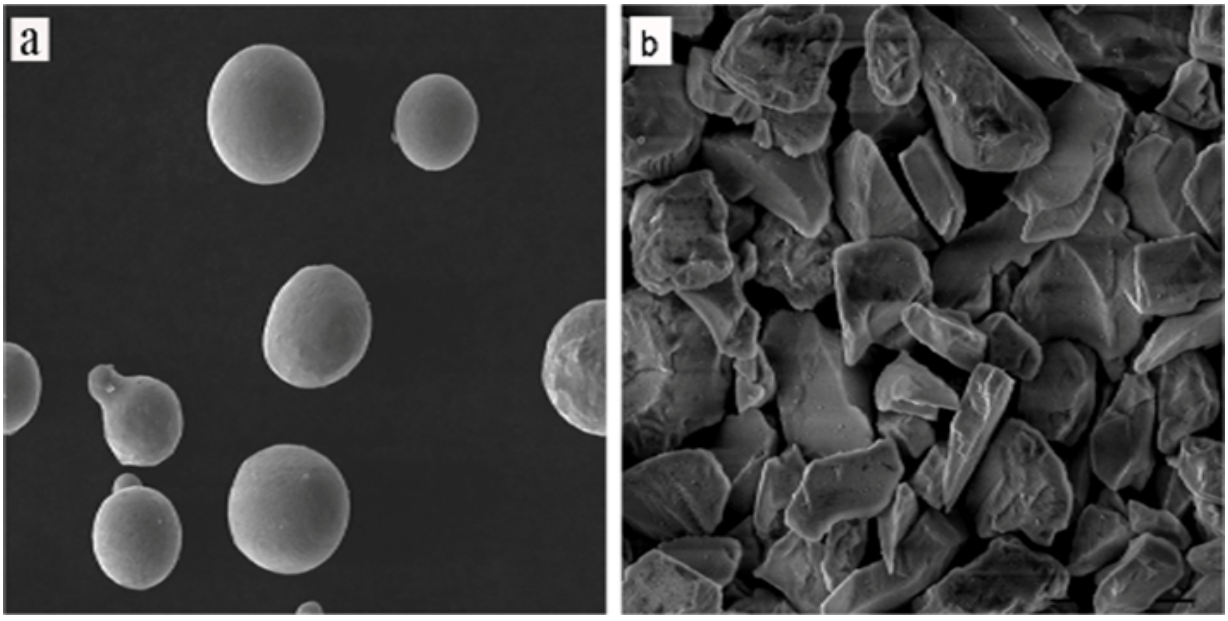

Figure 1: Powder pictures (a)NiCr powder; (b)Al_2O_3 powder

Table 1: Spraying parameters

Spraying parameters	NiCr	Al_2O_3
Main gas flow Ar (L/min)	130	110
Secondary air flow H_2 (L/min)	6.4	14.2
Spraying current (A)	380	400
Spraying voltage (V)	150	160
Spraying distance (mm)	110	90
Delivery amount (g/min)	30	30

2 Experimental materials and methods

2.1 Coating preparation

Self-developed high efficiency supersonic plasma spraying system [10] was employed to prepare NiCr coating, Al_2O_3 ceramic coating with NiCr undercoating and Al_2O_3 coating on AISI 1045 steel substrate with dimension of 80mm×50mm×4mm. The powder morphology of NiCr and Al_2O_3 is shown in Figure 1. Prior to spraying, the surface of substrate was cleaned with an acetone solution and sand-blasted [11]. In this experiment, "#"spraying path was applied on the specimen. The spraying parameters are listed in Table 1.

2.2 Impact indentation and extraction of AE signal

In this experiment, the 120° cemented carbide indenter was impacted by the 1 Kg of mass, which freely fell from a height of 400mm. During the process, crack originated and the failure of the coating was induced. Since the indenter was small, it was necessary to make an indenter cover to fix it. The indenter should be connected closely with the indenter cover; in addition, sliding or friction should be avoided. The bottom of weights and the top of indenter should be adhered by rubber with the thickness of 8mm in order to avoid interference signals produced by metal impact. In order to ensure the reliability of AE signals, a five-group impact indentation tests on each sample were conducted.

The process of impact indentation was monitored in real time by PCI -2 type AE monitoring equipment, which was produced by Physical Acoustics Corporation. The sensor probe and the sample surface was pasted closely by vacuum coupling agent The distance between probe and the impact point was about 15 mm, the model of sensor was Nano30, the gain of pre-amplifier was 40 dB, the software of data acquisition was AEwin, threshold value was 55 dB (only record the signals over more than 55 dB). The working principle of test equipment is shown in Figure 2. During the experiment, the sample need to be moved to the next position after a point signal has been collected.

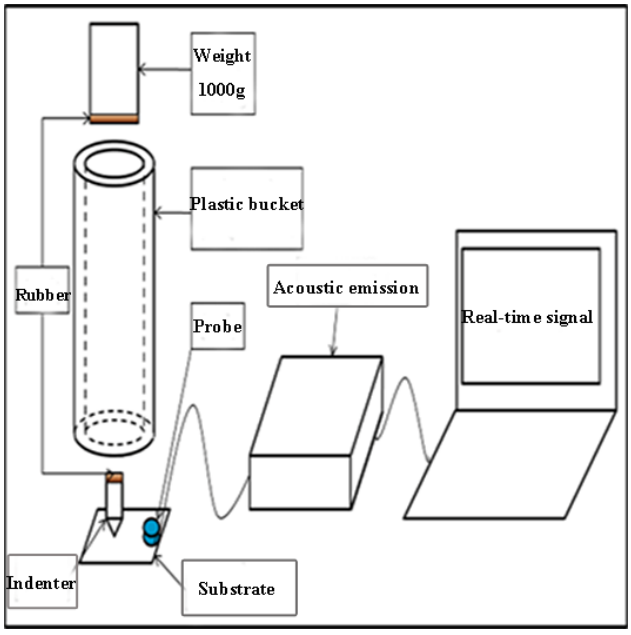

Figure 2: Schematic diagram of impact indentation method

2.3 Observation of indentation and treatment of AE signal

An scanning electron microscope (SEM) was used to observe the surface and cross section morphology of indentation. The 3D topography and dimension of the indentation were observed by a 3D profilometer. The AE signal data was processed by Origin software.

3 Experimental results and analysis

3.1 Analysis of indentation topography of the coating

3.1.1 SEM morphology of the coating indentation edge

Figure 3 shows the indentation surface morphology measured by SEM. It is shown that the indentation edges of substrate was more regular, while NiCr coating was slightly rough, and Al_2O_3 ceramic coating with NiCr undercoating was relatively coarse accompanied by cracking and spalling. But in terms of Al_2O_3 ceramic coating, there were large areas of spallings. The difference of indentation surface morphology of these four samples are due to the hardness of the substrate, NiCr coating, Al_2O_3 ceramic coating with NiCr undercoating and Al_2O_3 coating increased sequentially. Moreover, the bonding strength of them decreased successively [20].

The bonding strength of NiCr coating was better. The combination of Al_2O_3 ceramic coating with NiCr undercoating consists of two parts: one is the combination between NiCr undercoating and substrate, the other is the combination between NiCr undercoating and Al_2O_3 coating. As a whole, the combination of Al_2O_3 ceramic coating with NiCr undercoating was weaker than that of NiCr coating. As the bonding strength of hard coating can be improved effectively by the transition coating or undercoating [13], the bonding strength of Al_2O_3 ceramic coating with NiCr undercoating was higher than that of Al_2O_3 ceramic coating. By virtue of lower hardness and better plasticity, the edge of the substrate was relatively regular when impacted. NiCr coating owning higher hardness and lower plasticity than that of the substrate was liable to fracture at the edge of the coating, so the edge was a little coarse. The surface hardness of the Al_2O_3 ceramic coating with NiCr undercoating was higher and the plasticity was worse, so serious fracture was produced in the impact process, which led to rougher indentation edge. In addition, due to the bonding strength between the Al_2O_3 ceramic coating and NiCr undercoating is poor, a certain cracks appeared between the working coating and the transition coating, which led to a certain spalling at the edge of the indentation. Because of the bonding strength of the Al_2O_3 ceramic coating was very low, serious cracking occurred between the coating and substrate during the impact process, which eventually led to a large area of spalling at the edge of the indentation.

3.1.2 3D topography analysis of coating indentation

Figure 4 shows a 3D topography of indentation. It was evident that the indentation edge of the substrate was smooth, and there was almost no bulge, which was attributed to low hardness and good plasticity of the substrate. There was local bulge at the indentation edge of NiCr coating, and the reasons are as follows: firstly, the coating was subjected to impact indentation to produce plastic deformation, the internal coating of the indentation was extruded to the edge, thus a certain bulge was produced; secondly, cracking was produced between indentation edge of the coating and the substrate, which led to the tilting upwards and local bulge of the coating. A wide range of bulges emerged on the indentation edge of Al_2O_3 ceramic coating with NiCr undercoating. This was because the bonding strength between Al_2O_3 coating surface and NiCr undercoating was insufficient. A certain cracks and spallings between the coating and the undercoating were produced under impact indentation, which resulted in a

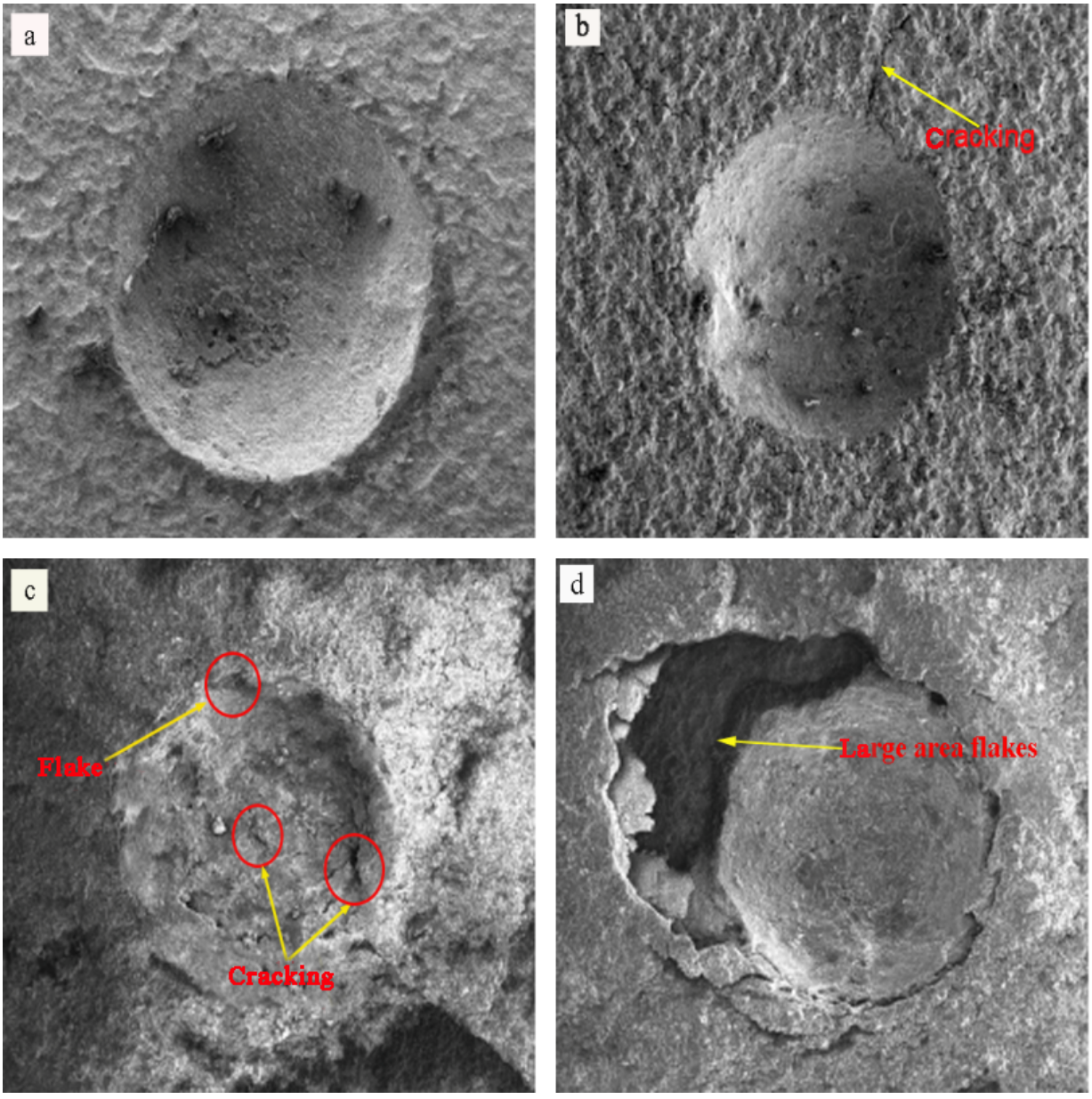

Figure 3: The surface morphology of indentation: (a)Substrate; (b)NiCr coating; (c)Al_2O_3 coating with the undercoating of NiCr; (d)Al_2O_3 coating

larger range of bulge at the indentation edge. The indentation edge of the Al_2O_3 ceramic coating had a wider range of bulges because there was no transition coating between Al_2O_3 coating and substrate, leading to a large area of cracking and spalling were produced between the coating and the substrate under impact indentation.

3.1.3 Indentation size analysis of coating

Table 2 shows the indentation size detected by the 3D profilometer. As shown in Table 2, Figure 3 and Figure 4, the indentation size of substrate, NiCr coating and Al_2O_3 coating with NiCr undercoating decreased in turn. The reason is the hardness of the substrate, NiCr coating and Al_2O_3 coating with NiCr undercoating increased in turn, which resulted in the indentation depth of indenter decreased in turn. Although the surface hardness of Al_2O_3 ceramic coating was the same as that of Al_2O_3 ceramic coating

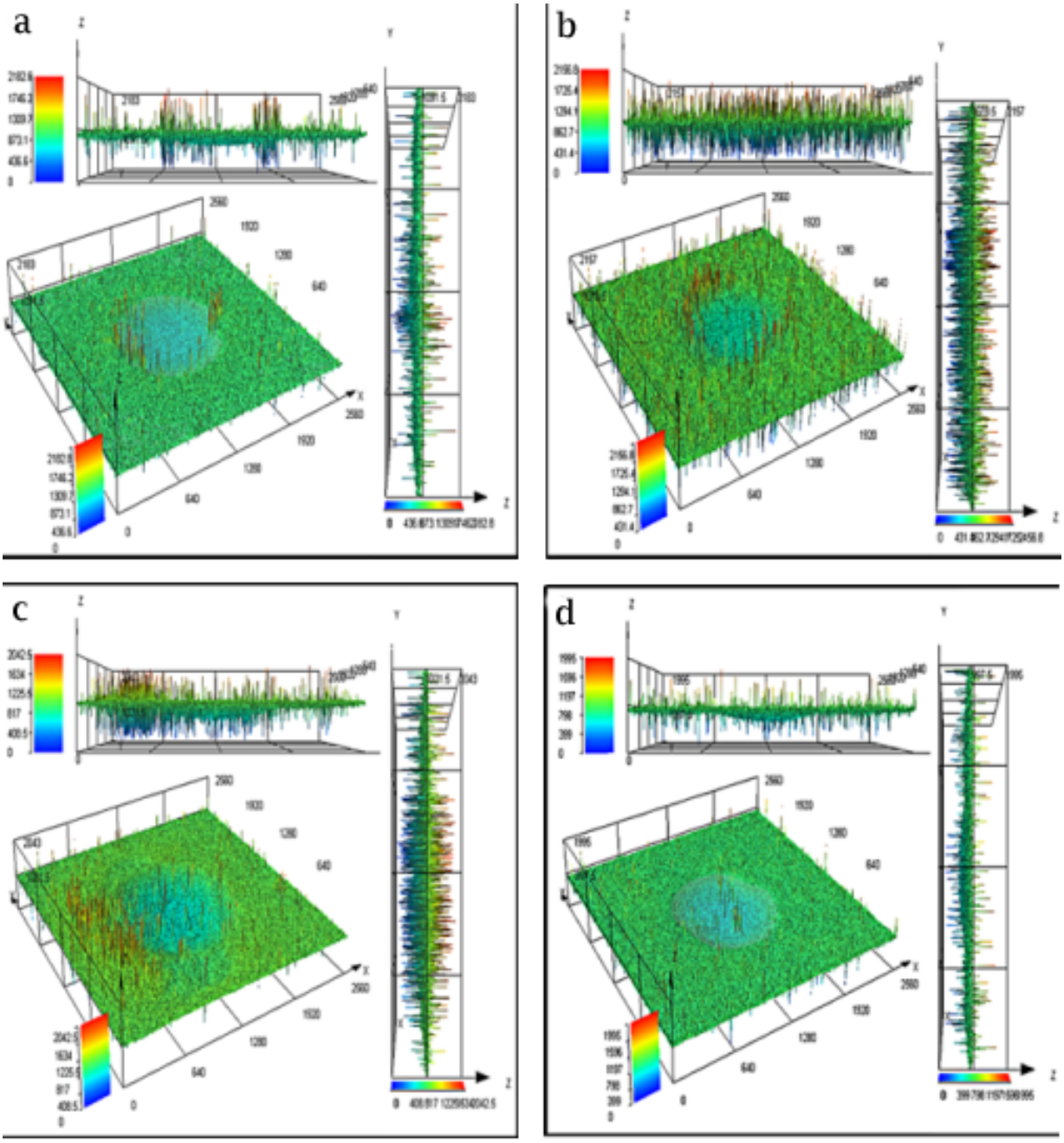

Figure 4: 3D topography of indentation: (a)Substrate; (b)NiCr coating; (c)Al_2O_3 coating with the undercoating of NiCr; (d)Al_2O_3 coating

with NiCr undercoating, the indentation size of the former was larger. The reason is that the poor bonding strength between the coating and the substrate led to the greater cracking tendency, which failed to provide greater resistance for the indenter.

3.1.4 Evaluation for bond strength of coating

Figure 5 shows a quality standard obtained from a German engineer manual to measure bonding strength of coatings by indentation method. In this figure, HF-1~HF-4 indicated that the bonding strength of the coating was sufficient, while HF-5~HF-6 indicated that strength was insufficient. If the indentation surface morphology and 3D topography of the coating in Figure 3 and Figure 4 were compared with the quality standard of bonding strength in Fig-

Table 2: Indentation dimensions of coating

Indentation dimensions	substrate	Metal coating	Ceramic coating	Bottomless ceramic coating
Diameters /mm	1.602	1.312	1.142	1.486
Depth/mm	0.414	0.346	0.303	0.472
Area/mm^2	1.424	1.092	0.930	1.326
Volume /mm^3	0.263	0.149	0.107	0.212

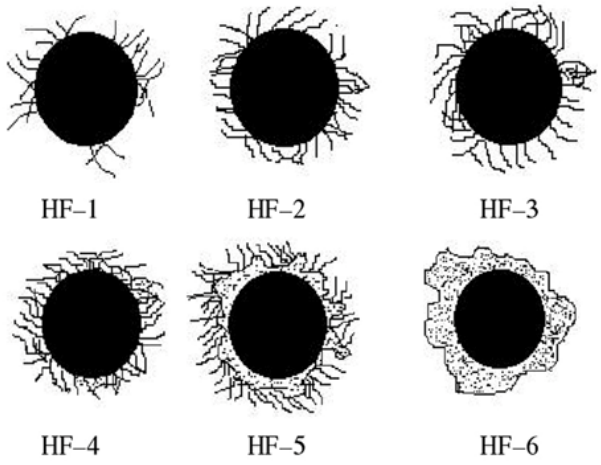

Figure 5: Quality standard for bond strength by indentation method

ure 5, it was found that the indentation morphology of the substrate was similar to HF-1, the NiCr coating was similar to HF-2, Al_2O_3 coating with NiCr undercoating was similar to HF-3 and HF-4, which indicating that all of these three kinds of coatings had sufficient bond strength. Their bonding strength in descending order is substrate, NiCr coating and Al_2O_3 coating with NiCr undercoating. But the indentation morphology of Al_2O_3 coating was similar to HF-5 and HF-6, hence its bonding strength was insufficient.

3.2 Mechanism analysis of coating cracking

Figure 6 shows the cross section of the micro-structure of the substrate, NiCr coating, Al_2O_3 coating with NiCr undercoating and Al_2O_3 coating, respectively. As indicated in the figure, there was no cracking in the substrate indentation, but a certain number of bulges could be observed. The reason is that the hardness of substrate was lower and the plasticity was better, which led to a larger plastic deformation when impacted. In the impact process, the substrate materials of indentation was extruded to the edge, and a certain bulges were produced (Figure 7). But owing to the degree of bulges were small, the bulges were difficult to be observed under SEM and 3D profilometer. Cracking was produced around the NiCr coating indentation, because the NiCr coating at the indentation edge uplifted during the impact process, which produced greater transverse shear stress and longitudinal tensile stress, and because of the low hardness and good plasticity of this metal coating, fracture was not easy to produce, but cracking occurred between the coating and the substrate. Both cracking and fracture were observed at the indentation edge of Al_2O_3 ceramic coating, the reason for which was the center of the indentation was subjected to greater impact compressive stress, and due to the Al_2O_3 coating possessed higher hardness and greater brittleness, fracture was produced under the stress. Because of the process of fracture is accompanied by a certain stress release, cracking was observed near the fracture position. There were three failure positions in Al_2O_3 coating with NiCr undercoating. The first was fracture of Al_2O_3 coating itself at the edge of indentation; the second was cracking between the surface Al_2O_3 coating and the NiCr undercoating near the edge of indentation; and the third was the cracking between the NiCr undercoating and the substrate around the indentation. The reason for that was the coating not only contains Al_2O_3 coating with higher hardness and greater brittleness, but also NiCr undercoating with low hardness and good plasticity. When they were subject to impact indentation stress, Al_2O_3 coating with higher hardness and greater brittleness would produce fracture, which resulted in stress release, so Al_2O_3 coating and NiCr undercoating cracked once again near the fracture position. At the same time; cracking appeared between the substrate and the NiCr undercoating with lower hardness and better plasticity under the action of transverse shear stress and longitudinal tensile stress.

3.3 Analysis of AE signal

3.3.1 Analysis of energy counting and amplitude

Figure 8 shows the AE signals of substrate, NiCr coating, Al_2O_3 coating with NiCr undercoating and Al_2O_3 coating

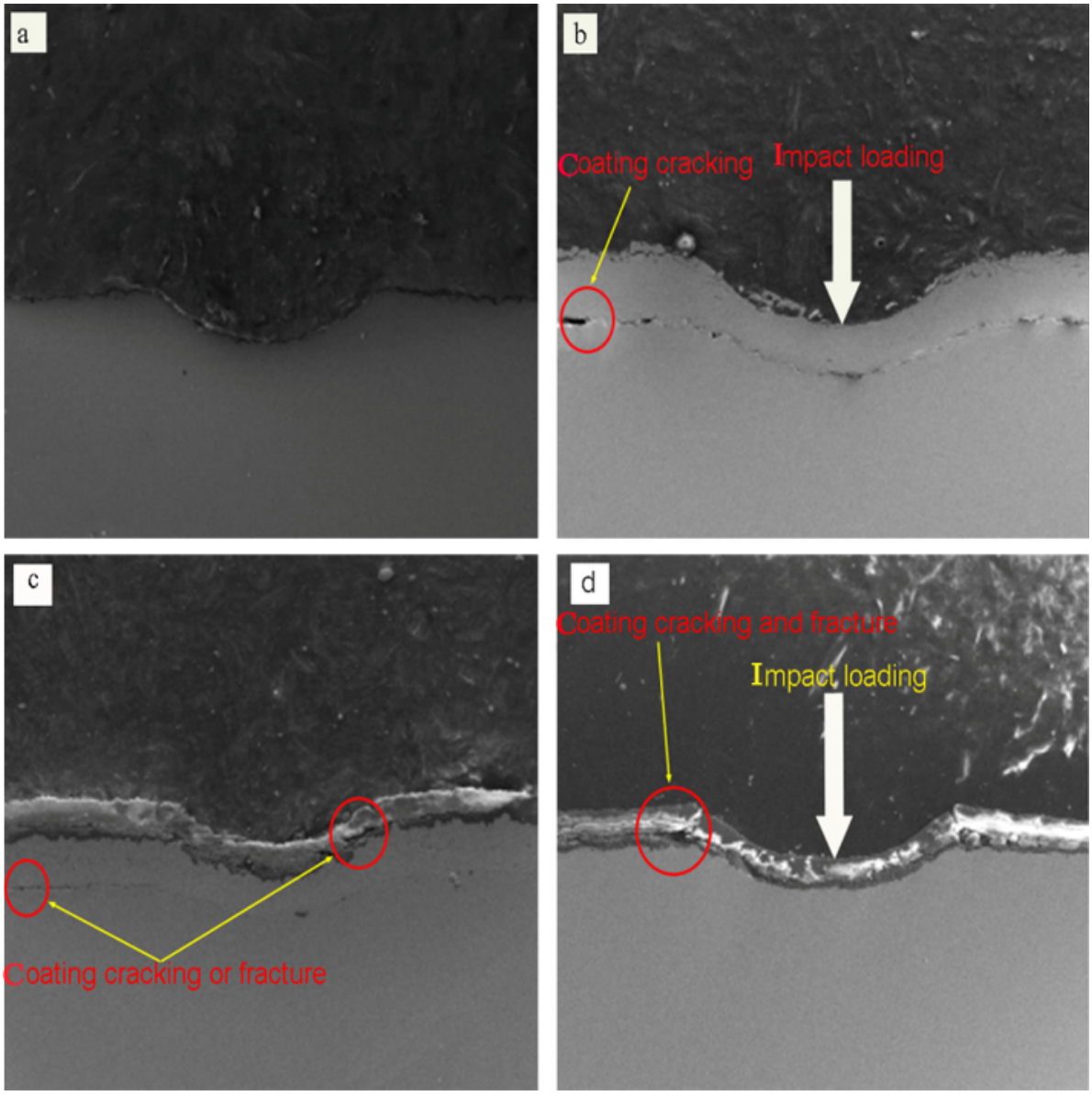

Figure 6: Micrograph of indentation section: (a)Substrate; (b)NiCr coating; (c)Al_2O_3 coating with the undercoating of NiCr; (d)Al_2O_3 coating

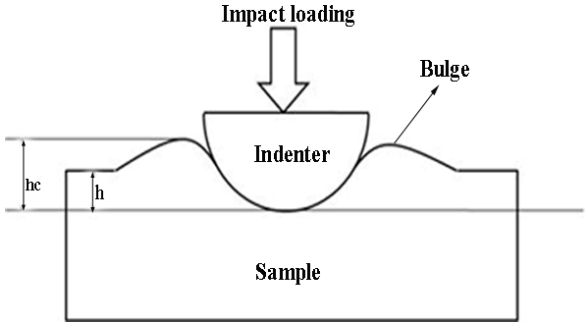

Figure 7: Cross-section of Indentation micromorphology

in the impact indentation process. The Y-axis represents AE energy counting and AE amplitude signal, and the X-axis represents time. As shown in the figure, the energy counting produced by the substrate was 400-800, and the amplitude was 70-90dB. There were a number of noise signals, which were from weight impacting the indenter, indenter impacting the substrate and the deformation of the substrate. During the impact process, the AE signals produced by the substrate can be used as a reference standard and compared with the AE signals produced by the coating. After the interference signals having been filtered out, the real cracking and fracture signals of the coating were extracted.

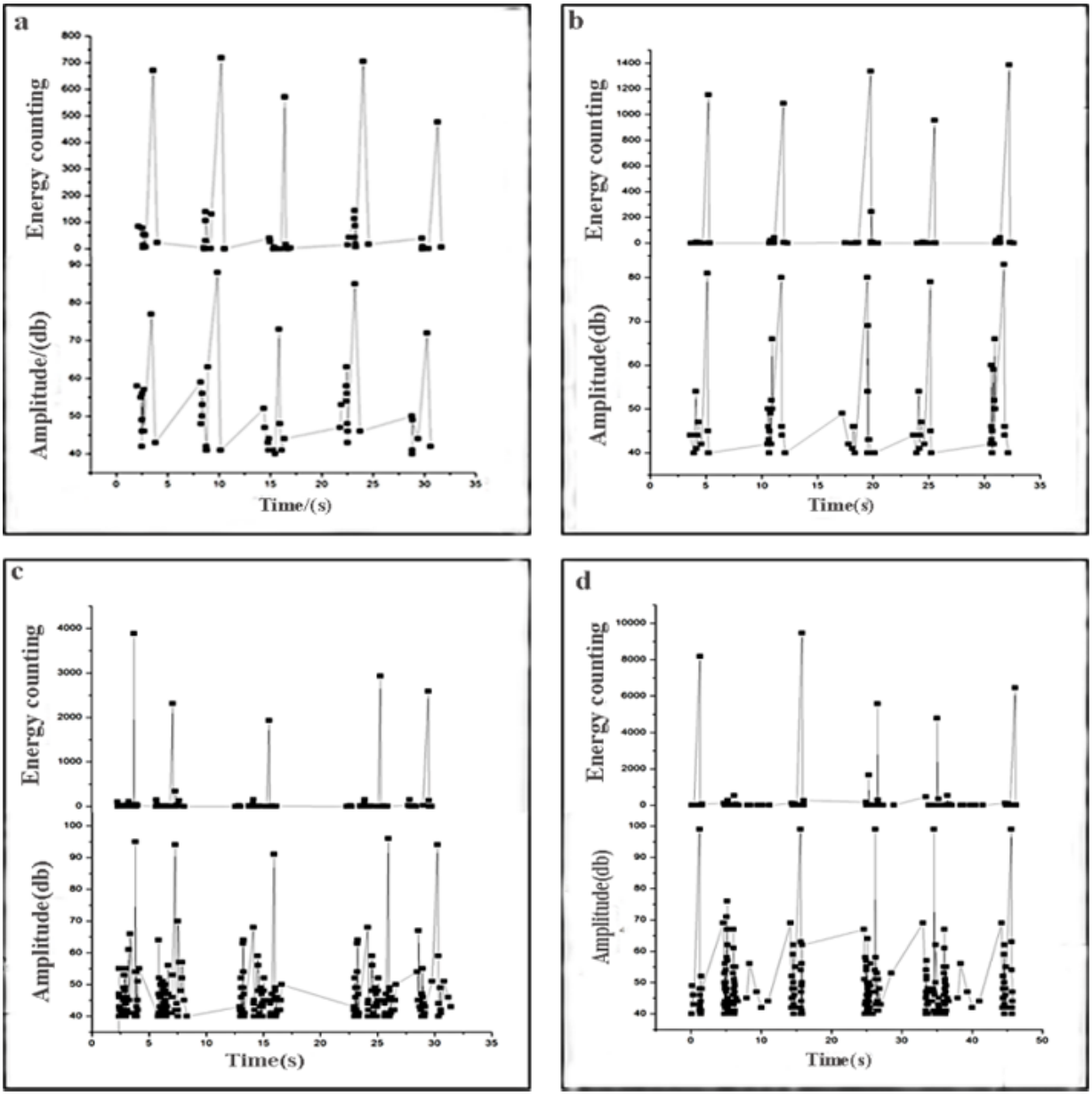

Figure 8: Acoustic emission(AE) signals analysis of coating: (a)Substrate; (b)NiCr coating; (c)Al_2O_3 coating with the undercoating of NiCr; (d)Al_2O_3 coatingtion SEM micromorphology

During the impact process, the energy counting of NiCr coating was about 1000~1500 and the amplitude was 80~85dB; Al_2O_3 coating with NiCr undercoating about 2000~4000, and the amplitude about 90~99dB; Al_2O_3 coating about 5000~10000 and the amplitude reached maximum, which was about 99dB. The energy counting of coatings were higher than that of substrate obviously and the higher part could be regarded as the signal of coating cracking and fracture. Compared with NiCr coating, the energy counting of Al_2O_3 coating was obviously larger. There were two reasons for this phenomenon: firstly, the hardness and brittleness of Al_2O_3 coating was larger, so the energy was larger during the impact process; secondly, the combination of the Al_2O_3 coating was poor and the cracking was more serious, so the energy counting was larger. Compared with the Al_2O_3 coating with NiCr undercoating, the energy counting of Al_2O_3 coating was more obvious although the hardness of them was identical. The reason was that the bonding strength of Al_2O_3 coating is lower, the cracking and fracture was more serious, so the energy counting was larger. Generally, in the impact process, the energy counting was affected by the bonding strength

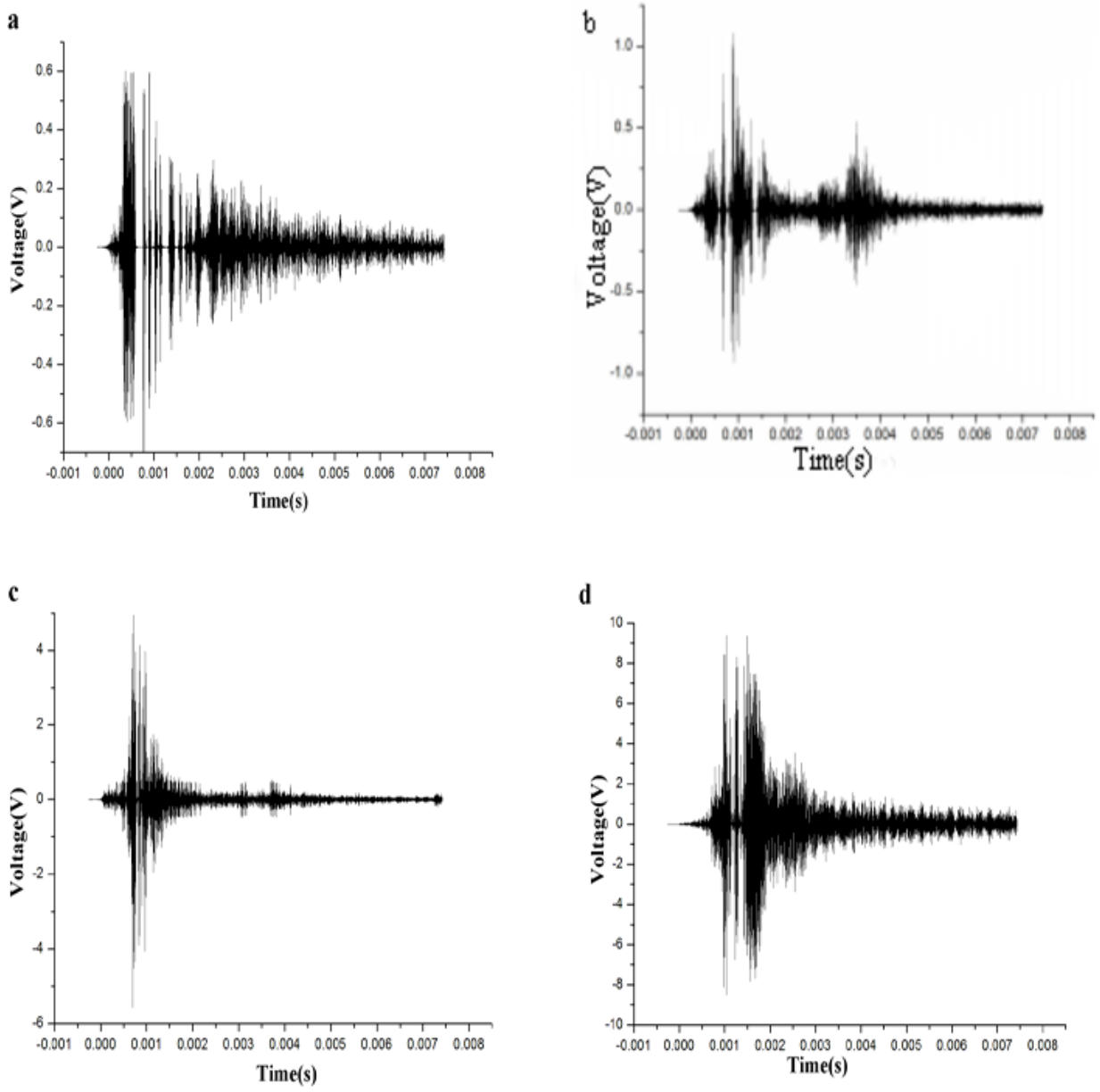

Figure 9: Spectrum analysis of coating: (a)Substrate; (b)NiCr coating; (c)Al_2O_3 coating with the undercoating of NiCr; (d)Al_2O_3 coating

and hardness of coating, but the bonding strength had a greater influence on the energy counting [20].

3.3.2 Analysis of wave voltage

Table 3 shows the wave voltage values of AE signals; the second wave of AE signals of each coating was extracted and was shown in Figure 9. It can be seen from Table 3 and Figure 9 that the wave voltage of substrate was about 0.4~0.7V, NiCr coating was about 1V, Al_2O_3 coating with NiCr undercoating was about 4~6V, and the Al_2O_3 coating reached the highest value, which was about 9~9.9V. The reasons for the difference of wave voltages was similar to that of energy counting. To some extent, the wave voltage was affected by hardness of the coating, but it mainly affected by bonding strength. The bonding strength of substrate, NiCr coating, Al_2O_3 coating with NiCr undercoating and Al_2O_3 coating decreased gradually, the cracking and fracture degree of coating increased successively, so the stress wave in the process of cracking and fracture increased in turn, and the wave voltage of the corresponding AE signals increased in turn as well.

Table 3: Waveform voltage values of AE signals

Test count	waveform voltage (V)			
	substrate	NiCr coating	Al_2O_3 coating	bottomless Al_2O_3 coating,
1	0.72	1.3	4.5	9.7
2	0.58	1.1	5	10
3	0.42	0.9	5.2	9.1
4	0.7	1.1	6.3	10
5	0.58	1.2	4.3	9.9

When comparing the bonding strength and AE signals of the above four samples, it was evident that the bonding strength of them decreased in turn, but the AE signals increased in turn, among which the energy counting and wave voltage were more sensitive to the variation of bonding strength [11]. So it can be concluded that the bonding strength of the coating was related to energy counting and wave voltage of AE signals, and the greater the bonding strength of the coating was, the smaller will be the energy counting and wave voltage.

4 Conclusions

In this paper, the bonding strength of NiCr coating, Al_2O_3 coating with NiCr undercoating and Al_2O_3 coating were studied using impact indentation method, whereupon the relationship between the failure mechanism of coatings and acoustic emission signal characteristics under impact condition was studied. The following conclusions can be drawn:

1 Through analysis of the surface morphology and 3D topography of the indentation, it was found that the cracking and spalling degree of substrate, NiCr coating, Al_2O_3 coating with NiCr undercoating and Al_2O_3 coating at the edge of indentation increased sequentially, and the bond strength reduced successively.
2 The analysis of micromorphology of the indentation section shows that local cracking of the interface or internal coating could be effectively induced by impact indentation method, and the cracking mechanism of these coatings are different. The failure mode of NiCr coating was dominated by interface cracking, and that of Al_2O_3 coating is fracture and is accompanied by a small amount of interface cracking, while Al_2O_3 coating with NiCr undercoating possesses common characteristics of the first two.
3 The bonding strength of the coating was related to AE signal produced in the impact process. The greater the bonding strength of the coating was, the smaller were the energy counting, the amplitude and the wave voltages. The energy counting and wave voltage were more sensitive to the variation of bond strength, which were suitable for characterizing the bond strength of coatings.
In a word, the impact indentation method accompanied with acoustic emission technology is feasible to characterize the bonding strength of the coating in the field.

Availability of data and materials: All data generated or analyzed during this study are included in this published article and its supplementary information files.

Competing interests: The authors declare that they have no competing interests.

Funding: This work was supported by the National Natural Science Foundation of China (Grant No. 51675158 and No. 51535011) and Natural Science Foundation of Hebei Province (Grant No. E2016202325)

Authors' contributions: D-TS analyzed the results and wrote the manuscript. W R and L-GL reviewed the whole manuscript and both made significant revisions. L M raised the basic concept of this work. W R provided the real worn surfaces data. D-TS and L]L provided the method of processing the surfaces data with bi-Gaussian method. M-HJ conducted the revising of the Gaussian acoustic emission model. D-TS overall instructed this research.

Acknowledgement: The authors gratefully acknowledge the financial supports of National Natural Science Foundation of China (51675158) and Natural Science Foundation of Hebei Province (E2016202325).

References

[1] L. J. Gu, Surf. Coat. Technol., 206 (2012) 4403-4410.
[2] J. Stallard, S.Poulat, and D. G. Teer, Tribol. Int. 39(2006)159-166.
[3] H. Zhang and D. Y. Li, Surf. Coat.,155 (2002) 190-194.
[4] S. Q. Guo, Scripta Materialia, 53 (2005) 1043-1048.
[5] Y. N. Song, Acta Acustica, 38 (2013) 413-418.
[6] H. J. Wang, Transactions of Materials and Heat Treatment, 35 (2014) 190 -194.

[7] Y. N. Song, Surface Engineering, 30 (2014) 675-682.
[8] H. J. Wang, Practical technology of thermal spraying, National Defense Industry Press, Beijing, China.
[9] H. J. Wang, R. C. Pan, and Z. H. Han, Heat Treatment of Metals, 05 (2005) 16-19.
[10] J. J. Kang, Tribol. Int, 73 (2014) 47-56.
[11] L. Ma, S. Low, and J. Song, Mechanics of Materials, 69 (2014) 213-226.
[12] G. Michlmayr, A. Chalari, A. Clarke and D. Or, 14 (2017) 1139-1146.
[13] Z. Y. Piao, B. S. Xu, H. D. Wang, Tribol. Int, 43 (2010) 252-258.
[14] L. Lin, J. J. Kang, T. S. Dong, Vacuum, 117 (2015) 40-46.
[15] J. J. Kang, Tribol. Int, 66 (2014) 249-258.
[16] J. J. Kang, Tribol. Int, 73 (2014) 128-137.
[17] Z. Y. Piao, Fusion Engineering & Design, 88 (2013) 2933-2938.
[18] T. Varis, T. Suhonen, Surf. Coat, 305 (2014) 123-131.
[19] D.Wen, Ceramics International, 43 (2017) 6976-6986.
[20] D. Bian, Ceramics International, 41 (2015) 9088-9092.